Theoretical Analysis of Beams Combining Ultra High Strength Concrete and Normal Strength Concrete

Ahmed M. Ismail,
Ph.D. student, Faculty of Engineering, Cairo University
Dr.Mohamed M.EL- Attar,
Professor Structural Engineering Department, Faculty of Engineering, Cairo University, Cairo, Egypt
Dr.Hossam Z. El-Karmoty
Professor, Housing and Building National Research Center, Cairo, Egypt.

Abstract:
In general, the structural engineer should concentrate towards the structural as well as functional design of the structure. So by keeping in mind the structure safety and economy, lead us to the concept of "Composite structures or partial elements. The basic idea for this concept is combining the normal strength concrete and UHSC or any recent advanced cementitious material in composite structures in order to exploit the advantages of the two materials in an optimal way. Recently Ultra-high Strength concrete (UHSC) is the most famous advanced cementitious materials that have exceptional properties, however their material costs are significantly higher than those of normal strength concretes. UHSC is characterized by extraordinary mechanical and durability properties, The UHSC-Matrix is very brittle material behavior, and it provides flexural strengths up to 50 MPa and compressive strengths up to 200 MPa. This research is considered a supplement research for an experimental previous one that was carried out in parallel by the same author [1]. It mainly aims to predict theoretically the behavior of the UHSC, NSC and composite concrete beams similar to the previous experimental program tested specimens, under the effect of the same parameters. This prediction was carried out by simulation of three models by using the first principle concepts. The materials which were used were the Ultra-High Strength Concrete (UHSC) (141MPa) and Normal strength concrete. By using the three simulated models a comparison between the theoretical beams behavior and the experimentally tested beams behavior was presented, in order to confirm the validity of these three models upon UHSC and Composite concrete beams. The previous experimental program was consists of ten reinforced concrete beams. The main parameters of this program were: longitudinal reinforcement ratio, the type of used concrete and the thickness of UHSC layer. A small parametric study was carried out through a prediction of another 12 beams that weren't tested experimentally, in order to confirm one of the previous experimental research related to the optimum use of the UHSC thickness layer in concrete. Finally, the three models give an acceptable prediction for each of NSC, UHSC and composite concrete beams. This models leads to the same Valuable conclusions that were obtained previously. It was concluded that in case of high reinforcement steel ratios the optimum thickness of UHSC in the concrete beams cross section should be not less than the third of the cross section depth only in order to achieve the economic point of view. In contrast, of the low reinforcement steel ratio the UHSC layers thickness can be decreased more than the third cross section depth.

Keywords:
Ultra High Strength Concrete, Composite, Normal strength concrete, Beams, Flexural behavior

Paper received 15th February 2018, Accepted 13th March 2018, Published 1st of April 2018

INTRODUCTION
In general and as mentioned above the UHSC material costs are significantly higher than those of normal strength concretes, so in order to optimize the uses of the UHSC in concrete beams the concept of composite "UHSC-concrete" structures can be applied to new structures and to conservation projects. Consequently it is well demonstrated that any typical composite elements whether slabs or beams consisting of reinforced cementitious materials in which it composed of a reinforced old concrete layer known as substrate and a new layer of an advanced cementitious material. This new layer is either thin less than 5 cm for the sake of rehabilitation or thicker than 5 cm to about 15 cm for improvement and increasing the element resistance [2]. It was previously denoted that the contribution of UHSC or Ultra-High-Strength Fiber-Reinforced Concrete

in the composite beams increases their stiffness and ultimate resistance than the RC elements alone. Also it was observed that the addition of a tensile R-UHPFRC reinforcement can be used as an effective shear strengthening method [3]. Furthermore, it was demonstrated that using the UHPFRC layers in concrete elements extend their durability due to the low permeability and tensile strain hardening properties of UHPFRC. The incorporation of rebar in the UHPFRC layer leads to a further increase in resistance and stiffness of the composite element and to a higher apparent magnitude of hardening in the UHPFRC. The investigated composite elements show monolithic behavior under service conditions [2].

A great Advance in the science of concrete materials in the past years have led to a new and modern development in the concrete technology. Mechanical properties and durability of concrete were facilitated by the sustainable use of supplementary materials and revolutionary developments in super plasticizing. For example the use of mineral and chemical admixtures, applying pre-setting pressure and using post setting heat treatment can be used to produce dense microstructure. These new advanced materials should exhibit high strength and high performance, in addition to greater durability characteristics. Ultra-High Strength Concrete (UHSC) is one of the materials that were developed in recent years. It is also known as reactive powder concrete (RPC). This material possesses a compressive strength greater than 21,750 psi (150 MPa).[4].

It must be highlighted that the previous researches and studies proved that the compressive strength was the only relevant factor for the development of the ultra-high strength concrete. While for the deformation behavior, the modulus of elasticity was only of secondary interest [5]. Shah.et.al 1998, [6] stated that, as the strength of the concrete increases, the material is more homogeneous; however it also becomes more brittle. Unreacted cement and aggregate particles produce significant heterogeneities in the standard high strength system, while the UHSC system is much more uniform at the same scale. In addition from many previous researches it was deduced that steel fibers which known as one of the UHSC mixes materials that sometimes can be used, have acquired significant popularity for use in concrete at relatively low volume fractions. They are the optimal for using in improving the flexural strength, toughness and resistance, to shrinkage-induced cracking. [7]

The main objective of this research is to propose three models for the prediction of structural flexural behavior for each of NSC, UHSC (141MPa) and composite concrete beams by using the concrete first principal concept. In addition to using these models to confirm a previous experimental program results that also study this behavior under different parameters under static loads. Also both the current theoretical study confirm the main target of the previous experimental program which was represented in reaching to optimum thickness of ultra-high strength concrete layer in composite beams according to the steel reinforcement ratios of the concrete beams.

RESEARCH PROGRAM

This paper presents a simulation for three models to predict analytically the structural behavior of NSC, UHSC and composite concrete beams by using the reinforced concrete first principals concept and also a confirmation for a previous experimental program results was carried out by using these three models. This previous experimental program was carried out to investigate the different parameters that affect the of UHSC and composite beams using Ultra High Strength Concrete (UHSC) (141MPa) and Normal strength concrete under the effect of static loads; in this ten beams were included and designated as B1 to B10 and subjected to concentrated loads. These beams divided into three groups composed of two NSC beams, five composites beams and three UHSC beams. All of these ten beams have a length of 6000 mm and a cross section of 300×150 mm. A clear cover of 15 mm was provided to all test specimens. Two types of concrete were used in casting these eleven beams Ultra high strength Concrete with a target compressive strength about (141MPa) and Normal Concrete(NSC) with a target compressive strength (30 MPa) .The studied parameters that affect the behavior, ductility, Toughness and stiffness of the tested beams include the type, thickness of concrete and the longitudinal steel reinforcement ratio. Tables (1) show the configurations of experimental program of the ten specimens. In addition, Figure (1) shows the concrete dimensions and steel reinforcement details of specimen B1 and finally Figure (2) show the experimental program test setup and it instrumentations.

Table 1: Beams Configurations

Specimen	UHSC thickness (cm)	NSC thickness (cm	Type of concrete	Main Reinforcement	% ρ	Stirrups
B1	0	30	normal	6Φ16	3.17	10Φ10/m
B2	30	0	ultra	6Φ16	3.17	10Φ10/m
B3	10	20	Composite	6Φ16	3.17	10Φ10/m
B4	30	0	ultra	6Φ18	4.03	10Φ10/m
B5	30	0	ultra	6Φ22	6.13	10Φ10/m
B6	10	20	Composite	6Φ18	4.03	10Φ10/m
B7	10	20	Composite	6Φ22	6.13	10Φ10/m
B8	7	23	Composite	6Φ22	6.13	10Φ10/m
B9	5	25	Composite	6Φ22	6.13	10Φ10/m
B10	0	30	normal	4Φ16	2.11	10Φ10/m

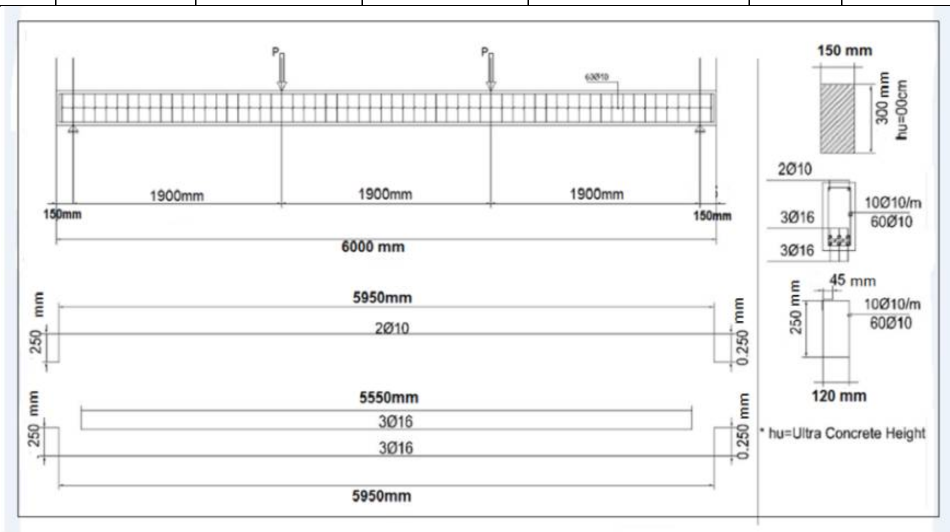

Fig.1: the concrete dimensions and steel reinforcement details of specimen B1

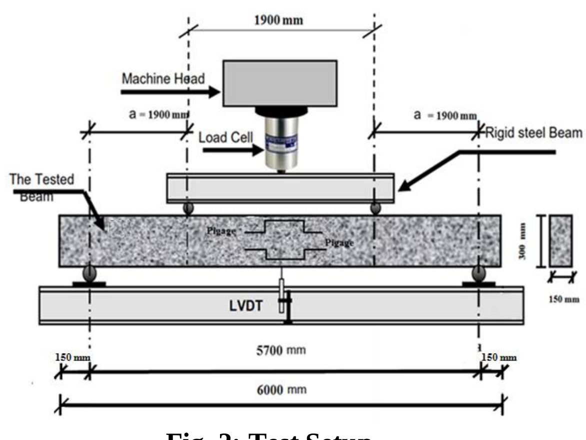

Fig. 2: Test Setup

MATERIALS and ASSUMPTION MODELING

The three models were simulated based on neglecting the effect of concrete in tension. The materials, which were used to simulate these theoretical models, were Normal strength concrete, Ultra High strength concrete and steel reinforcement in which their properties and characteristics are expressed as the following:

NORMAL STRENGTH CONCRETE:

The stress-strain relationship of the Normal strength concrete was modeled using a parabolic relationship in compression as illustrated in Figure (3). Instead of using the parabolic stress distribution, the internal compression force in the concrete was evaluated using an equivalent uniform stress distribution with stress-block factors γ and β as shown in Figure (4). For a given parabolic compression stress distribution, γ and β were calculated such that the magnitude and location of the resultant force did not change. The maximum concrete strain in the compression was measured and was found to be 0.0035. The elastic modulus of concrete E_{CN} that was determined based on control specimens of concrete was equal to 24 Gpa. The concrete strain ε_c' corresponding to the maximum stress was related to the measured concrete strength f_c and elastic modulus in compression E_{CN} as ($\varepsilon_c' = 2\, f_C / E_{CN}$).

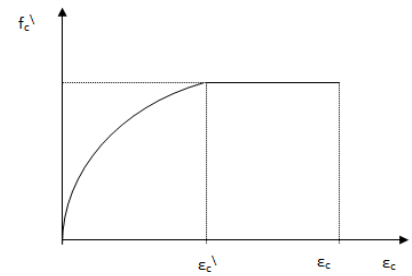

Fig. 3: Idealized stress-strain curve of concrete in compression

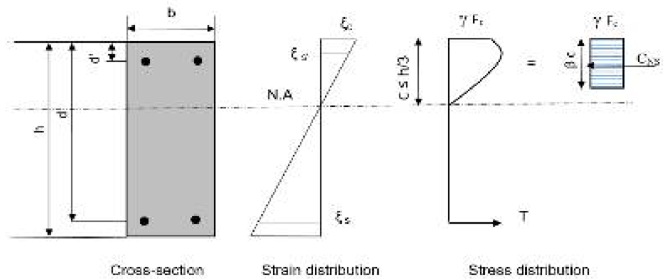

Fig.4: Analysis of a Rectangular Section for Normal strength Concrete

ULTRA-HIGH STRENGTH CONCRETE

A linear relationship was used to model the UHSC stress-strain relationship as illustrated in Figure (5). The linear stress distribution is represented by a triangular stress block as shown in Figure (6). The resultant force of this triangular stress block Fc was maintained using the $F_c = 0.5 f_c\, b\, c$

Refering to Khattab 2010 [8], the maximum compression strain ε_c in UHSC was about 0.003 to 0.0035. In addition, the elastic modulus E_{CU} of (UHSC) was taken to be 38.6 Gpa based on Khattab 2010 research results on a group of UHSC specimen.

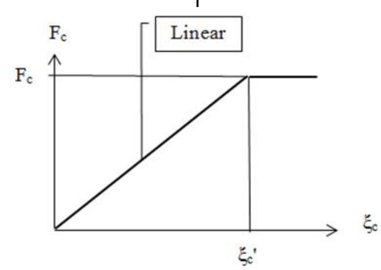

Fig.6: **Analysis of a Rectangular Section for UHSC**

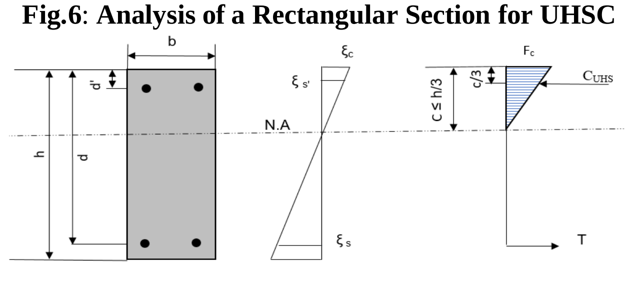

Fig.5: **Idealized Stress-Strain Curve of Concrete UHSC in Compression**

COMPOSITE CONCRETE:

It is well demonstrated that the composite section in this study include two different types of concrete mixes UHSC and NSC. The UHSC mix is used in the compression zone or a part of it up to a certain thickness (hu) which is considered one of the parameters that chosen to carry out this study, while the second concrete type which is the NSC is used in the tension zone. Figure (7) show the stress-strain relationship of the composite concrete and it was denoted that it is nearly similar to the stress-strain relationship of the UHSC, see Fig (5 & 7).

The internal compression force in the composite concrete can be evaluated by using the stress distribution as shown in Figure (7&8). This can be applicable only when the distance from the top of compression fiber to the neutral axis (C) is greater than UHSC thickness (hu), such that the internal compression force will be obtained through the resultant of two forces; the force of the UHSC thickness (C_{UHSC}) and the internal force of the NSC thickness (C_{NSC}). But when the distance from the top of compression fibre to the neutral axis (C) be smaller than UHSC thickness (hu), the internal force can be evaluated by using the linear stress distribution as illustrated in Figure (6). So a theoretical model was simulated to analyze the composite section. This model have a valid prediction until the compression depth (C) decreasing continually to reach the value of UHSC thickness (hu), consequently the concrete compression block will be only one type of concrete which is UHSC which is automatically analyzed by the UHSC model instead of the composite model.

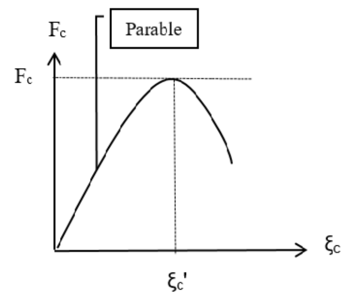

Fig.7: Idealized Stress-Strain Curve Of Composite Concrete In Compression

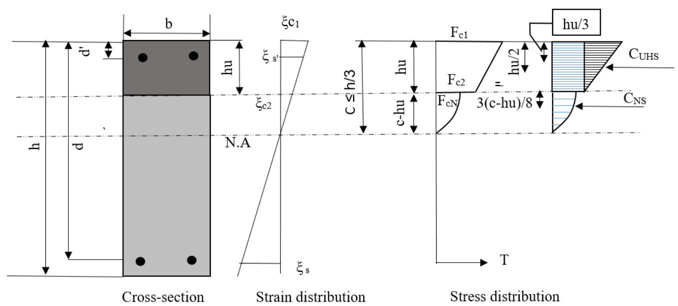

Fig.8: Analysis of Composite Concrete Rectangular Section

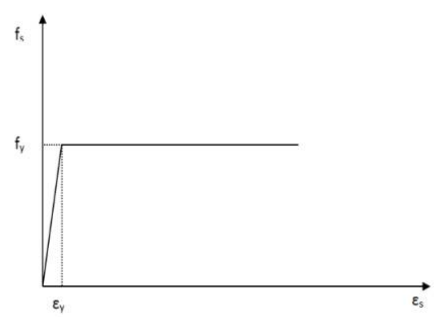

Fig.9: Idealized Stress-Strain Curve of Steel in Tension And Compression

STEEL REINFORCEMENT

Deformed high tensile steel of 16, 18 and 22 mm diameter and yield strength of 450 KN/mm^2 and ultimate strength of 630 KN/mm2 were used as a main tension reinforcement for all tested beams. While deformed high tensile bars of 10-mm diameter, yield strength 420 KN/mm2 and ultimate strength 630 KN/mm^2 were used for closed stirrups. The idealized shape of the stress-strain curve of steel reinforcement consisted of two straight lines, as given in Figure (9), ignoring the increase of the stresses after yield and strain hardening.

1. MODELS CALCULATIONS AND ASSUMPTIONS:

Calculation of Moment-Curvature Relationship and Deflection Prediction:

Moment- Curvature Relationship:

Two assumptions were considered the first one that the Plain cross sections remain plain after deformation, which means that the strain is linearly distributed over the cross section and implies complete bond between the materials. The second one is that the cracked concrete has no tensile strength. Consequently, the procedure of each type of concrete beams NSC, UHSC and composite concrete cross sections was derived according to the equilibrium and strains compatibility equations (see Table2). These equations were obtained from stress and strain distributions that illustrated in figures (4, 6 and 8). Then by substituting in the equilibrium and strains compatibility equations, the compression depth (c) was derived in the form of a second-degree equation, which is a function in (ε_C). Thus, a series of iteration was developed to calculate the moment-curvature relationship at the critical section. In which a certain values for the concrete compressive strain at the extreme fiber ε_c was assumed, then the corresponding values of compression depth (c) were obtained and also the corresponding curvature, strains, stresses and forces in concrete and steel reinforcement are calculated. It is well demonstrated that there are four cases were taken into consideration in these calculations. These cases differs according to the steel strain in both tension and compression zones as shown in table (3).

Table 2: Equilibrium and Strains Compatibility Equations for UHSC, NSC and Composite beams cross sections

Concrete Type	**Analysis Equations**	
	Strain Compatibility	Force Equilibrium
Normal Strength Concrete Sections	**- $\varepsilon_s = \varepsilon_c$ [(d-c) /(c)]** **- $\varepsilon_s' = \varepsilon_c$ [(c-d')/(c)]**	**- $C_N = \gamma\beta F_c$ c b = $A_s F_s$ - $A_s' F_s'$**
Ultra-High Strength Concrete sections	**- $\varepsilon_s = \varepsilon_c$ [(d-c)/(c)]** **- $\varepsilon_s' = \varepsilon_c$ [(c-d')/(c)]**	**- C_U = 0.5 F_c c b = $A_s F_s$ - $A_s' F_s'$**
Composite Concrete Sections	**- $\varepsilon_s = \varepsilon_{c1}$ [(d-c)/(c)]** **- $\varepsilon_s' = \varepsilon_{c1}$ [(c-d')/(c)]** **- $\varepsilon_{c2} = \varepsilon_{c1}$ [(c-h_u)/(c)]**	**- $C_U + C_N = A_s F_s - A_s' F_s'$** **- C_U = [($F_{c1} + F_{c2}$)/2] (h_u b)** **- C_N = 0.667(c – h_u) F_{cN} b ➡ parabolic shape**

Table 3: Compression Depth (c) Equations for the simulated models

Type of Concrete Section	**Case1** *(Both top and bottom longitudinal steel before reaching yield stress)*	**Case 2** *(top longitudinal steel at yield stress)*	**Case 3** *(Both top longitudinal steel at yield stress)*	**Case 4** *(Both top and bottom longitudinal steel after reaching yield stress*
Normal Strength Concrete	$\left(\left(\frac{1}{\varepsilon_c{}'}\right) - 0.333\left(\frac{\varepsilon_c}{\varepsilon_c{}'2}\right)\right) F_c b\, \mathbf{c}^2 + (A_s E_s + A_{s'} E_{s'})\boldsymbol{c} - (A_s E_s d + A_{s'} E_{s'} d') = 0$	$\left(\left(\frac{1}{\varepsilon_{c'}}\right) - 0.333\left(\frac{\varepsilon_c}{\varepsilon_{c'2}}\right)\right) F_c b\, \boldsymbol{c}^2 + \left(A_{s'} E_{s'} - \frac{A_s F_y}{\varepsilon_c}\right)\boldsymbol{c} - A_{s'} E_{s'} d' = 0$	$\left(\left(\frac{1}{\varepsilon_c{}'}\right) - 0.333\left(\frac{\varepsilon_c}{\varepsilon_c{}'2}\right)\right) F_c b\, \mathbf{c}^2 + \left(A_s E_s + \frac{A_{s'} F_y}{\varepsilon_c}\right)\boldsymbol{c} - A_s E_s d = 0$	$\mathbf{c} = \frac{A_s F_y - A_{s'} F_y}{\gamma\beta F_c b}$
Ultra High Strength Concrete	$0.5 E_c b\, \mathbf{c}^2 + (A_s E_s + A_{s'} E_{s'})\boldsymbol{c} - (A_s E_s d + A_{s'} E_{s'} d') = 0$	$0.5 E_c b\, \boldsymbol{c}^2 + \left(A_{s'} E_{s'} - \frac{A_s F_y}{\varepsilon_c}\right)\boldsymbol{c} - A_{s'} E_{s'} d' = 0$	$0.5 E_c b\, \mathbf{c}^2 + \left(A_s E_s + \frac{A_{s'} F_y}{\varepsilon_c}\right)\boldsymbol{c} - A_s E_s d = 0$	$\mathbf{c} = \frac{A_s F_y - A_{s'} F_y}{0.5 E_c \varepsilon_c b}$
Composite Concrete	$0.667\varepsilon_{c1} E_{cN} b\, \mathbf{c}^2 + [\varepsilon_{c1} h_u b\,(E_{cu} - 1.333 E_{cN}) + \varepsilon_{c1}(A_s E_s + A_{s'} E_{s'})]\boldsymbol{c} + [\varepsilon_{c1} h_u{}^2 b\,(0.667 E_{cN} - 0.5 E_{cU}) - A_s E_s \varepsilon_{c1} d - A_{s'} E_{s'} \varepsilon_{c1} d'] = 0$	$0.667\varepsilon_{c1} E_{cN} b\, \boldsymbol{c}^2 + [\varepsilon_{c1} h_u b\,(E_{cu} - 1.333 E_{cN}) - A_s F_y + A_{s'} E_{s'} \varepsilon_{c1}]\boldsymbol{c} + [\varepsilon_{c1} h_u{}^2 b\,(0.667 E_{cN} - 0.5 E_{cU}) - A_{s'} E_{s'} \varepsilon_{c1} d'] = 0$	$.667\varepsilon_{c1} E_{cN} b\, \boldsymbol{c}^2 + [\varepsilon_{c1} h_u b\,(E_{cu} - 1.333 E_{cN}) + A_{s'} F_y + A_s E_s \varepsilon_{c1}]\boldsymbol{c} + [\varepsilon_{c1} h_u{}^2 b\,(0.667 E_{cN} - 0.5 E_{cU}) - A_s E_s \varepsilon_{c1} d] = 0$	$.667\varepsilon_{c1} E_{cN} b\, \boldsymbol{c}^2 + [\varepsilon_{c1} h_u b\,(E_{cu} - 1.333 E_{cN}) - A_s F_y + A_{s'} F_y]\boldsymbol{c} + [\varepsilon_{c1} h_u{}^2 b\,(0.667 E_{cN} - 0.5 E_{cU})] = 0$

A sequence of iterations was carried out for solving these previous equations, this sequence of iterations stopped when concrete reaches its ultimate strain in compression. Finally, the ultimate moment M and curvature ∅ of critical sections are calculated as follow:

For Normal Strength Concrete sections:

$$M = \gamma\beta F_c\, b\, c\,(d - 0.5\beta c) + A_{s'} F_{s'}(d - d')$$

For Ultra-High Strength Concrete sections:

$$M = 0.5F_c\, b\, c\left(d - \frac{c}{3}\right) + A_{s'} F_{s'}(d - d')$$

For Composite Concrete sections:

$$M = F_{c2} b\, h_u\,(d - 0.5h_u) + (F_{c1} - F_{c2})0.5b\, h_u\left(d - \left(\frac{h_u}{3}\right)\right) + F_{cN}(c - h_u)0.667b\left(d - h_u - \left(\frac{3(c - h_u)}{8}\right)\right) + A_{s'} F_{s'}(d - d')$$

The curvature ∅ will be calculated

$\emptyset = (\varepsilon_c - \varepsilon_s)/d$

DEFLECTION PREDICTION:

In general the deflection was calculated using integration of the curvature at many sections along the beam span. The curvature was calculated using strain compatibility approach as described previously. For each load increment, the moment-curvature relationship at deferent sections along the length of the beam was determined. The deflection was calculated by integration of the curvature from the joint to the mid-span section to obtain the maximum deflection due to the specified load. The curvature integration was performed numerically using the following equation and as illustrated in Figure (10).

$$\Delta = \Sigma\ (\Phi i\ Xi + \Phi i{+}1\ Xi{+}1)\ \Delta\ Xi\ /\ 2$$

The deflection was determined by integration of the curvature at five distinct sections. In general, the sections should be selected at any expected abrupt change of the curvature. The selected sections were at the supports, cracking moment, yield moment, location of the concentrated load and mid-span as shown in Figure (11).

$$\Delta = \{(\Phi_1 X_1 + \Phi_2 X_2)\ \Delta X_1 / 2\} + \{(\Phi_2 X_2 + \Phi_3 X_3)\ \Delta X_2 / 2\} + \{(\Phi_3 X_3 + \Phi_4 X_4)\ \Delta X_3 / 2\} + \{(\Phi_4 X_4 + \Phi_5 X_5)\ \Delta X_4 / 2\}$$

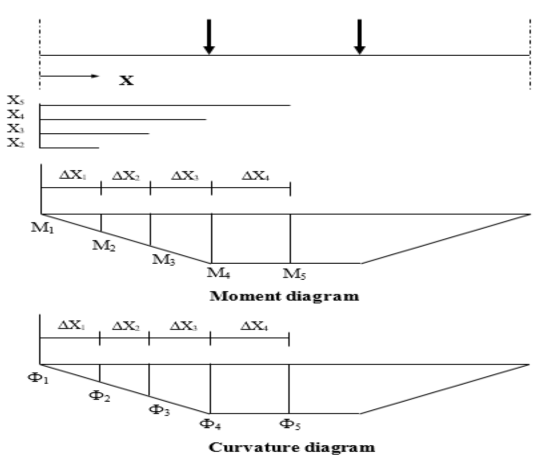

Fig.10: Numerical Integration of the Curvature For Deflection Calculation

MODELS EVALUATIONS AND RESULTS DISCUSSIONS

A comparison study is conducted to verify the theoretical calculations with the previous experimental results and to validate the applicability of the three simulated models. The comparison concentrated on some of the important aspects such as: the load-deflection and the moment-curvature responses. Table (4) show the values of the maximum capacity of beams experimentally and theoretically also this table show the ductility values resulted from experimental test versus the theoretical models analysis.

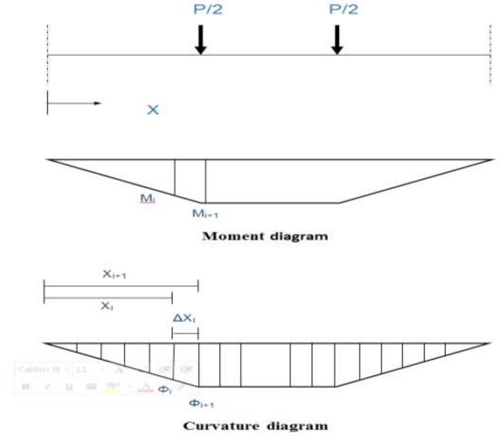

Fig.11: Numerical Integration of the Curvature at Key Sections

Consequently, Figures from (12) to (21) show a comparison between, load-deflection relationship resulted from experimental and theoretical analysis, for all the tested beams and simulated models. In addition, the predicted moment-curvature relationships for beams B1, B2, B3 and B4 only were illustrated through Figures from (22) to (24).

In general, through the shown figures, it was concluded that the three simulated models give a good prediction for the behavior of each of NSC, UHSC and composite concrete beams.

In addition, by referring to figures (19 and 20), it was denoted that these models are invalid only for beams B8 and B9 that represents two composite beams that have an UHSC thickness less than the third cross section depth, 70 and 50 mm respectively with the same longitudinal reinforcement ratio (6.13%). In these beams, the compression depth (C) value at the maximum load is larger than the value of UHSC thickness (hu) which cause an increase in the obtained theoretical maximum load value than its experimental corresponding value. This can be explained that the compression block of concrete at failure, will be composed of the two types of concrete, which need a broader, comprehensive and more detailed study.

Table 4: Experimental and Theoretical Analysis Results

Beam No	P_{max} Experimental (KN)	P_{max} Theoretical (KN)	Ductility Experimental	Ductility Theoretical
B1	110	104.58	1.82	1.65
B2	146.1	140.05	2.20	2.17

B3	141.1	140.05	1.95	1.89
B4	165.4	167.8	2.012	1.98
B5	266.6	231.4	1.120	1.004
B6	187.7	167.8	1.94	1.75
B7	257.6	231.42	1.1	1.15
B8	218.8	227.20	1.04	1.20
B9	188.2	206.45	1.02	1.14
B10	85.6	82.6	2.86	2.75

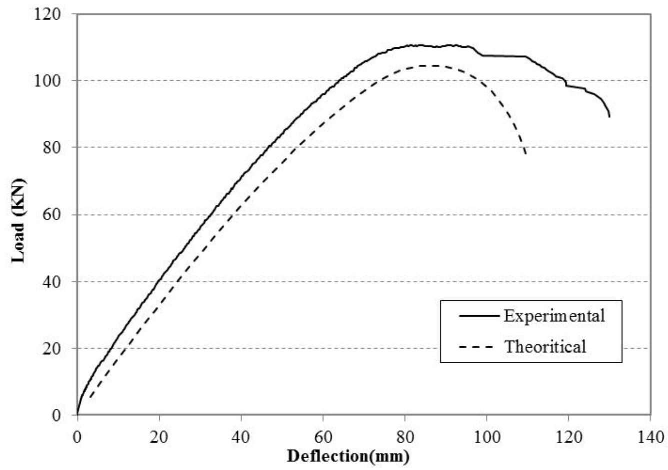

Fig.12: Experimental and Theoretical Load deflection curve for B1

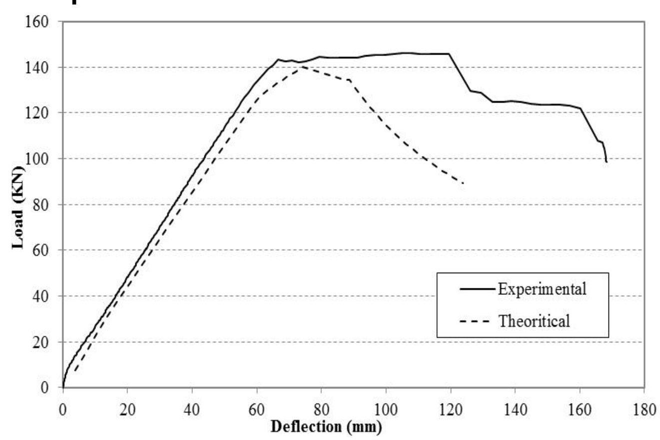

Fig.13: Experimental and Theoretical Load deflection curve for B2

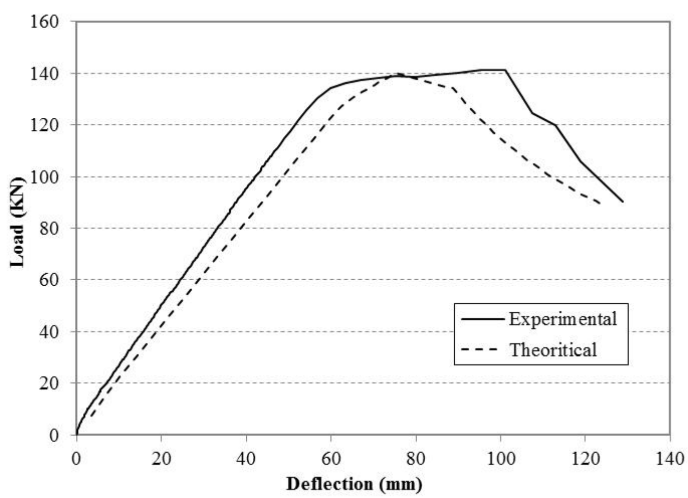

Fig.14: Experimental and Theoretical Load deflection curve for B3

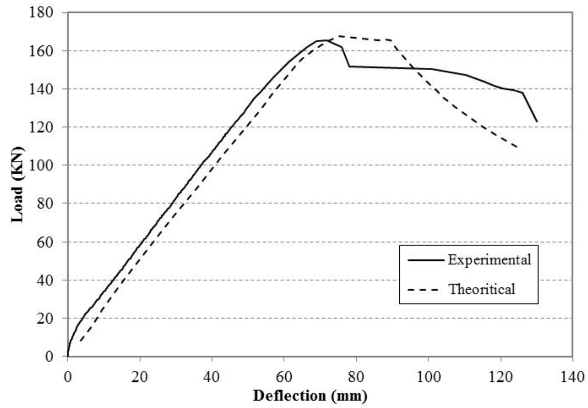

Fig.15: Experimental and Theoretical Load deflection curve for B4

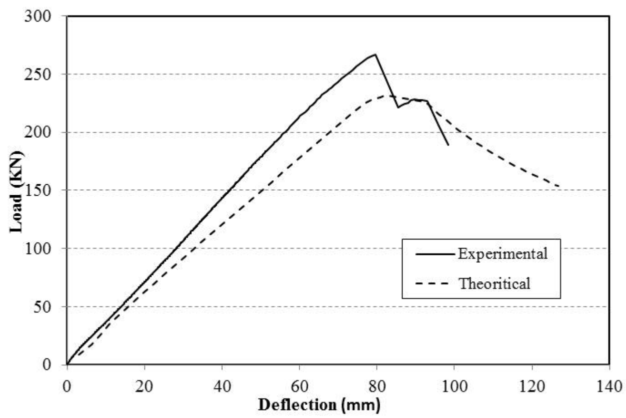

Fig.16: Experimental and Theoretical Load deflection curve for B5

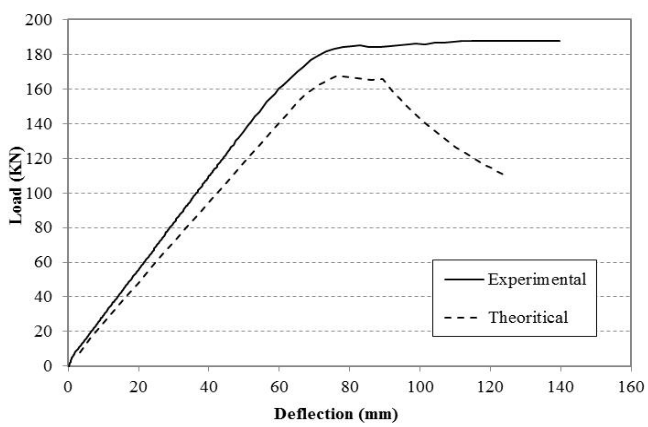

Fig.17: Experimental and Theoretical Load deflection curve for B6

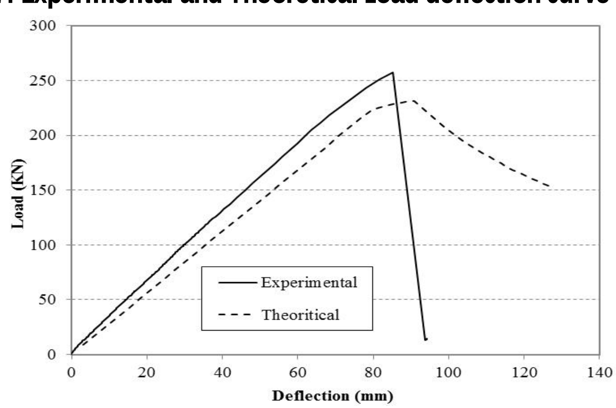

Fig.18: Experimental and Theoretical Load deflection curve for B7

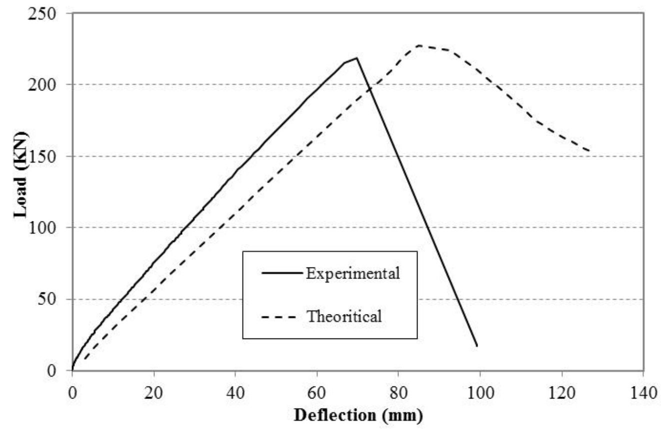

Fig.19: Experimental and Theoretical Load deflection curve for B8

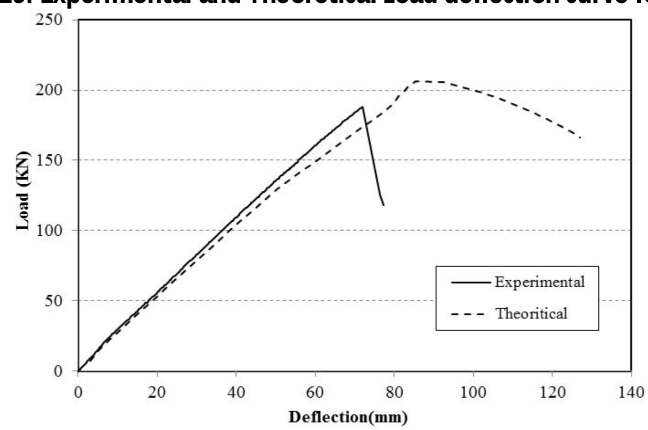

Fig.20: Experimental and Theoretical Load deflection curve for B9

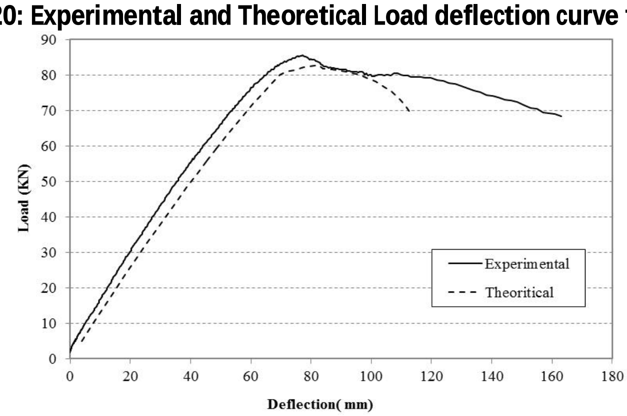

Fig.21: Experimental and Theoretical Load deflection curve for B10

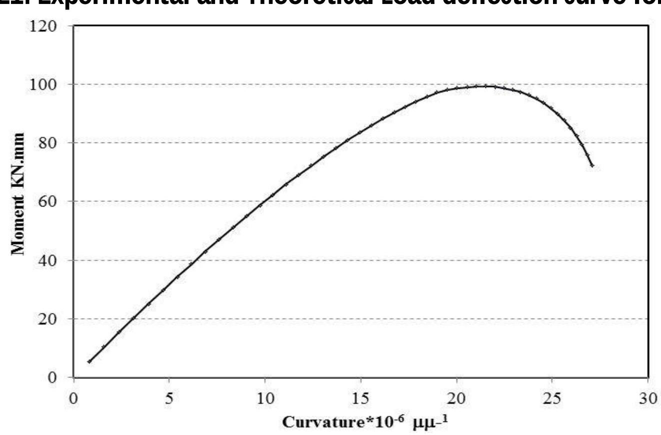

Fig.22: Moment Curvature Relationship for B1

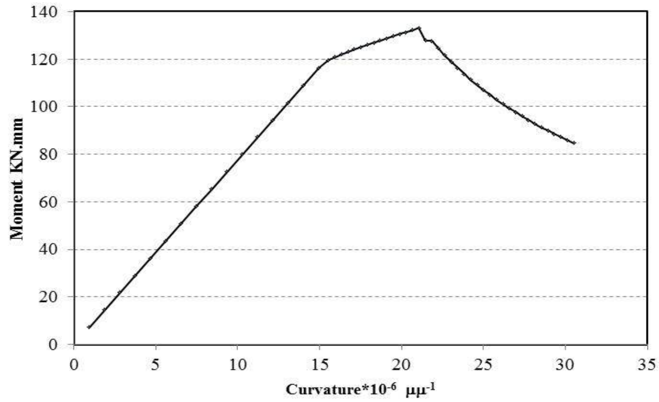

Fig.23: Moment Curvature Relationship for B2

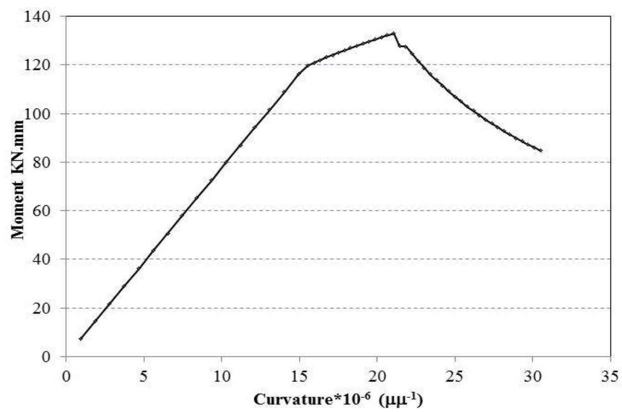

Fig.24: Moment Curvature Relationship for B3

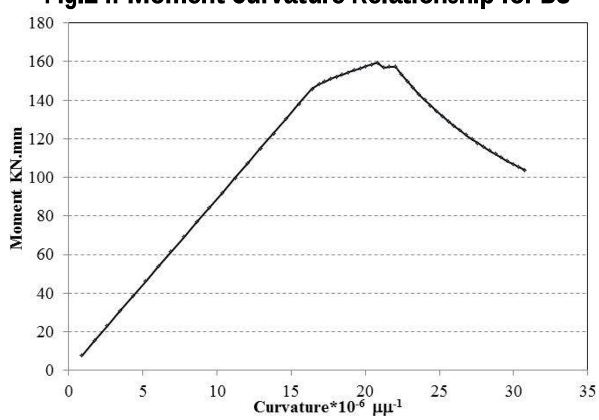

Fig.25: Moment Curvature Relationship for B4

Additional Parametric Study:

An additional parametric study was carried out to predict theoretically the behavior of some beams that were not tested experimentally. It aims to confirm the main conclusion of the previous experimental research that is mainly related to the effect of both longitudinal reinforcement steel ratio and the UHSC thickness. This parametric study divided into five group of beams that include 20 beams. Eight of them have similar corresponding beams that were tested experimentally, in addition to 12 beams that were analyzed theoretically to be a supplement of these groups, as shown in tables (5). Each group of these beams have the same reinforcement ratio but have a different thickness of UHSC layer in order to study its effect on the beams behavior.

Table 5: Beams Configurations for the additional parametric study.

Group No	Specimen	UHSC thickness (cm)	NSC thickness (cm)	Type of concrete	Main Reinforcement Ratio (ρ %)	Notes

1	B2	30	0	ultra	3.17	*These beams have a corresponding similar beams that were tested experimentally*
	B3	10	20	Composite		
	B11	7	23	Composite		*These beams weren't tested experimentally*
	B12	5	25	Composite		
2	B4	30	0	ultra	4.03	*These beams have a corresponding similar beams that were tested experimentally*
	B6	10	20	Composite		
	B13	7	23	Composite		*These beams weren't tested experimentally*
	B14	5	25	Composite		
3	B5	30	0	ultra	6.13	*These beams have a corresponding similar beams that were tested experimentally*
	B7	10	20	Composite		
	B8	7	23	Composite		
	B9	5	25	Composite		
4	B15	30	0	ultra	8.02	*These beams weren't tested experimentally*
	B16	10	20	Composite		
	B17	7	23	Composite		
	B18	5	25	Composite		
5	B19	30	0	ultra	10.19	
	B20	10	20	Composite		
	B21	7	23	Composite		
	B22	5	25	Composite		

Additional Parametric Study Results:

The results of the parametric study is illustrated through table (6) that include the values of both compression depth (C) and Compression strain in concrete ε_c at the maximum load (Pmax) for each group. Consequently, a comparison of each group of beams was carried out by plotting their load deflection relationships as shown in Figures (26, 27, 28 and 29).

From the shown Figures and tables, it was observed that in case that the compression depth (C) at the maximum load (Pmax) is less than or equal to the UHSC thickness (hu) all the compression zone will be UHSC only. Therefore, the simulated model for composite concrete section will not be valid and consequently the resulted maximum load values will be very convergent or nearly the same values. This mentioned case achieved in the parametric study through group1 (B2, B3 and B11), group2 (B4 and B6) and finally in group3 (B5 and B7). However, in case that the compression depth (C) at the maximum load (Pmax) is greater than the UHSC thickness (hu) the simulated model for composite concrete section will be valid as shown in group1 (B12), group2 (B13 and B14), group3 (B8and B9) and finally all beams of gruoup4.

In addition, it is well demonstrated that for very high longitudinal reinforcement ratios, the simulated models will be invalid because the compression concrete strain will reach to the maximum values before yielding of tension steel is occurred, as in case of group 5 beams.

Table 5: Results of the additional parametric study

Group No	**Specimen**	**UHSC thickness h_u (cm)**	**Main Reinforcement & Ratio (ρ%)**	**Compression depth C (cm)**	**Compression strain in concrete ε_c**	**P max**	Notes
1	B2	30	6Φ16 (3.17%)	5.55	0.0031	140.0	When the compression depth at Pmax (C) $\leq h_u$ *the section will be fail at ultra-block only*
	B3	10		5.55	0.0031	140.0	
	B11	7		5.55	0.0031	140.1	
	B12	**5**		**5.74**	**0.003**	**138.71**	

2	B4	30	6Φ18 (4.03%)	7.28	0.003	167.8	When the compression depth at Pmax (C) $\le h_u$ *the section will be fail at ultra-block only*
	B6	10		7.28	0.003	167.8	
	B13	**7**		**7.27**	**0.003**	**167.68**	
	B14	**5**		**7.37**	**0.003**	**164.38**	
3	B5	30	6Φ22 (6.13%)	10.01	0.0033	231.4	When the compression depth at Pmax (C) $\le h_u$ *the section will be fail at ultra-block only*
	B7	10		10.01	0.0033	231.4	
	B8	**7**		**10.16**	**0.0033**	**227.20**	
	B9	**5**		**10.48**	**0.0033**	**206.45**	
4	B15	30	6Φ25 (8.02%)	13.14	0.0033	280.8	When the compression depth at Pmax (C) $\le h_u$ *the section will be fail at ultra-block only*
	B16	**10**		**13.26**	**0.0033**	**277.79**	
	B17	**7**		**13.67**	**0.0033**	**257.06**	
	B18	**5**		**14.11**	**0.0033**	**225.00**	
5	B19	30	6Φ28 (10.19%)	14.99	**0.0036**	304.2	The programs (Ultra & composite) aren't valid in case of (ρ = 10.19) because $\varepsilon_c \ge 0.0035$ (max. strain at failure)
	B20	10		15.15	**0.0037**	302.3	
	B21	7		15.21	**0.0038**	274.2	
	B22	5		13.37	**0.0044**	240.1	

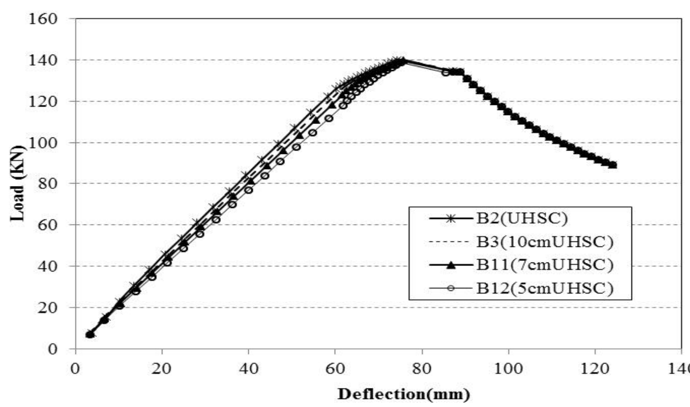

Fig.26: Theoretical Load deflection curve for B2, B3, B11 and B12

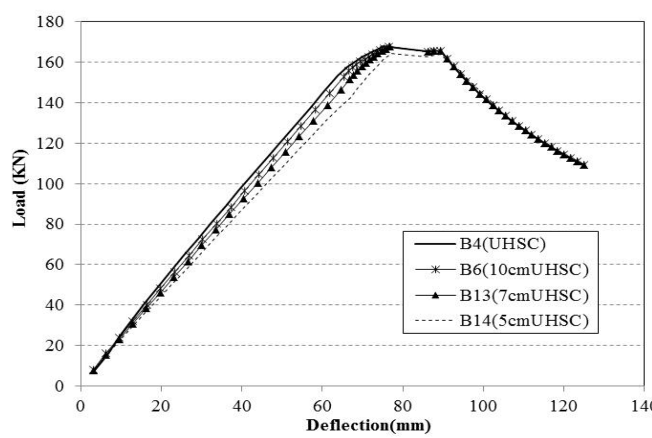

Fig.27: Theoretical Load deflection curve for B4, B6, B13 and B14

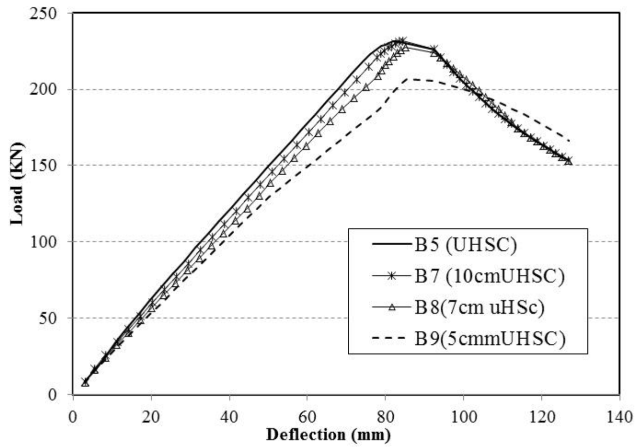

Fig.28: Theoretical Load deflection curve for B5, B7, B8 and B9

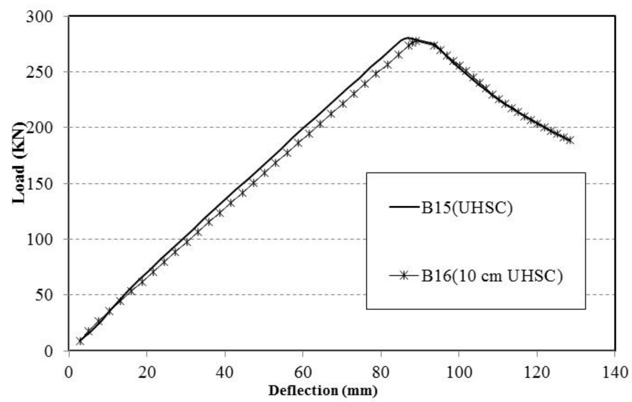

Fig.29: Theoretical Load deflection curve for B15, B16, B17 and B19

CONCLUSIONS

From the analysis and discussion of the test results obtained from this research, the following conclusions can be drawn.

1. The three simulated models give a good prediction for the behavior of each of NSC, UHSC and composite concrete beams that were tested experimentally. In case that the value of compression depth (C) at the maximum load is less than or equal to the value of UHSC thickness (hu).
2. For high reinforcement steel ratios, the thickness of UHSC layers cannot be decreased more than the third of cross section depth due to appearing of crushing in NSC layer before it appears in UHSC layer and before the reinforcement steel reaching the yield.
3. The obtained theoretical maximum load value will be larger than its experimental corresponding value, in case that the value of the compression depth (C) at the maximum load is larger than the value of UHSC thickness (hu), which need a broader, comprehensive and more detailed study.
4. For high longitudinal reinforcement ratios (10.18%), the simulated models will be invalid because the compression concrete strain will reach to the maximum values before yielding of tension steel is occurred
5. The Egyptian code for design and construction of concrete structures' limit for the beams maximum longitudinal steel reinforcement ratio is applicable in both UHSC and composite concrete beams. Consequently it will be sufficient to use the UHSC thickness equal to the third of the cross section depth.
6. By decreasing the reinforcement steel ratio, less than the maximum limit the UHSC layers thickness can be decreased more than the third cross section depth. But In this case a specialized consultant should be perform the required theoretical calculations.

REFERENCES

1. Ismail.A, El Attar.M and El karmouty.H "Structure Behavior of Beams Combining Ultra High Strength Concrete and Normal Strength Concrete", International design Journal, Accepted in January2018.
2. Katrin HABEL," structural behavior of elements combining ultra-high performance fibre reinforced concretes (UHPFRC) and reinforced concrete" 2004.

3. Noshiravani.T and Eugen Brühwiler.E, "Experimental Investigation on Reinforced Ultra-High Performance Fiber Reinforced Concrete Composite Beams Subjected to Combined Bending and Shear" ACI Structural Journal, V. 110, No. 2, March-April 2013.
4. Allena.S and Newtson.M, "Ultra-High Strength Concrete Mixtures Using Local Materials", Concrete sustainability conference 2010, National Ready Mixed Concrete Association- New Mexico State University.
5. Webe.D and Jianxin.M ," Mechanical Properties Of Ultrahigh Strength Concrete", LACER No. 8, 2003.
6. Shah.S and Weiss.W," Ultra High Strength Concrete : A Look To The Future" , The Zia Symposium, ACI Spring convention ,1998.
7. Bahaa. T.,"Seismic Behavior of Reinforced High Strength Concrete Beam Column Joints With and Without Steel Fiber", PHD. Thesis, Faculty of Engineering, Cairo University, 2002.
8. Khattab.E , June 2010 " Production of Ultra high strength concrete using local materials and its application in axially loaded columns", PHD Thesis, Faculty of engineering ,Ain Shams university.
9. Pai, S. D., Munshi, V. G. and Ukidve, A. V. Seam quality of cotton threads. Textile Asia, 1984, 15(6), 80-81.